HHS Public Access

Author manuscript

Nat Cell Biol. Author manuscript; available in PMC 2014 June 01.

Published in final edited form as:

Nat Cell Biol. 2013 December ; 15(12): 1464–1472. doi:10.1038/ncb2868.

The physiological role of mitochondrial calcium revealed by mice lacking the mitochondrial calcium uniporter (MCU)

Xin Pan[1,2,*], **Jie Liu**[1,*], **Tiffany Nguyen**[3,*], **Chengyu Liu**[4], **Junhui Sun**[3], **Yanjie Teng**[1], **Maria M Fergusson**[1], **Ilsa I Rovira**[1], **Michele Allen**[5], **Danielle A. Springer**[5], **Angel M. Aponte**[6], **Marjan Gucek**[6], **Robert S. Balaban**[3], **Elizabeth Murphy**[3,**], and **Toren Finkel**[1,**]

[1]Center for Molecular Medicine, National Heart, Lung and Blood Institute, National Institutes of Health, Bethesda, MD USA 20892

[2]National Center of Biomedical Analysis, Beijing, China 100850

[3]Systems Biology Center, National Heart, Lung and Blood Institute, National Institutes of Health, Bethesda, MD USA 20892

[4]iPSC and Genome Engineering Core, National Heart, Lung and Blood Institute, National Institutes of Health, Bethesda, MD USA 20892

[5]Murine Phenotyping Core, National Heart, Lung and Blood Institute, National Institutes of Health, Bethesda, MD USA 20892

[6]Proteomic Core, National Heart, Lung and Blood Institute, National Institutes of Health, Bethesda, MD USA 20892

Abstract

Mitochondrial calcium has been postulated to regulate a wide range of processes from bioenergetics to cell death. Here, we characterize a mouse model that lacks expression of the recently discovered mitochondrial calcium uniporter (MCU). Mitochondria derived from $MCU^{-/-}$ mice have no apparent capacity to rapidly uptake calcium. While basal metabolism appears unaffected, the skeletal muscle of $MCU^{-/-}$ mice exhibited alterations in the phosphorylation and activity of pyruvate dehydrogenase. In addition, $MCU^{-/-}$ mice exhibited marked impairment in their ability to perform strenuous work. We further show that mitochondria from $MCU^{-/-}$ mice lacked evidence for calcium-induced permeability transition pore (PTP) opening. The lack of PTP opening does not appear to protect $MCU^{-/-}$ cells and tissues from cell death, although $MCU^{-/-}$ hearts fail to respond to the PTP inhibitor cyclosporin A (CsA). Taken together, these results clarify how acute alterations in mitochondrial matrix calcium can regulate mammalian physiology.

**To whom correspondence should be addressed: Toren Finkel, NIH, Bldg 10/CRC 5-3330, 10 Center Drive, Bethesda, MD 20892, T: 301-402-4081, finkelt@nih.gov; Elizabeth MurphyNIH, Bldg 10/Rm 8N202, 10 Center Drive, Bethesda, MD 20892, T: 301-496-5828, murphy1@nih.gov.

*these authors contributed equally

The authors declare no competing financial interest.

Contributions: X.P, J.L and T.N. designed, performed and analyzed the experiments and aided in writing the manuscript, C.L. help construct the mouse model, J.S., Y.T., M.M.F., I.I.R., M.A., D.A.S., A.M.A, and M.G. contributed to the completion of various experiments, R.S.B, E.M and T.F. conceived the study, supervised the research and contributed to the writing the manuscript.

Calcium plays a central role in a diverse array of cellular processes including signal transduction, secretion of bioactive molecules, muscle contraction and gene expression. Over fifty years ago, it was demonstrated that fully energized mitochondria could rapidly sequester a large, sudden increase in intracellular calcium[1,2]. Calcium entry into this organelle requires that the ion traverses both the outer and inner mitochondrial membrane (IMM). Subsequent studies have demonstrated that passage of calcium through the ion-impermeable IMM requires the large membrane potential difference generated by the action of the electron transport chain[3]. Subsequent physiological and biophysical studies identified that large amounts of calcium could rapidly enter the mitochondrial matrix through this transport mechanism[4,5]. These observations, along with observations that entry of calcium was not directly coupled to the movement of another ion[6], established that mitochondrial calcium uptake occurred through a specific channel termed the mitochondrial calcium uniporter (MCU), that could bind calcium with nanomolar affinity[7]. While it was well known that the entry of calcium could be inhibited by the cell-impermeant compound ruthenium red[8], for nearly four decades the identification of this ruthenium red sensitive mitochondrial uniporter remained elusive. That situation changed when two groups recently reported the existence of a transmembrane protein CCDC109A that appeared to fulfill the requirement of the long elusive MCU protein[9,10]. These groups identified that MCU is a protein of approximately 40-kDa that is widely expressed and localizes, as expected, to the IMM[9,10].

Although the molecular identity of MCU was unknown until recently, the role of mitochondrial calcium has been intensively studied over the last four decades. These studies have collectively demonstrated that mitochondrial calcium acutely regulates a range of mitochondrial enzymes involved in either the supply of reducing equivalents [11], metabolic substrates [12] or electron transport[13]. Together, these observations supported the notion that MCU-dependent entry of calcium represented a central component of metabolic regulation. Indeed, it had been known that cells and tissues appear capable of exquisitely matching the rate of ATP production with ATP utilization such that even with large fluctuations in power output, levels of metabolic intermediates such as ATP, ADP and P_i appear unchanged[14,15]. This has been extensively studied in tissues such as the heart or skeletal muscle that see large and acute changes in their energy utilization when, for instance, the organism goes from a resting state to a full speed sprint. Under these conditions, it has been widely believed that the entry of mitochondrial calcium augments mitochondrial ATP production to acutely match the rapid increase in ATP demand[11,16-18].

While the entry of small amounts of calcium may have beneficial effects for metabolic homeostasis, there is a significant amount of data demonstrating that the uptake of large amounts of Ca^{2+} can induce cell death [19,20]. The basis for this phenomenon involves opening of the permeability transition pore (PTP). While the precise molecular makeup of the PTP has remained elusive, evidence suggest that the entry of calcium through an MCU-dependent mechanism is the central mediator of PTP opening [21-23]. Once opened, the PTP results in depolarization of the IMM leading to collapse of the mitochondrial membrane potential and thus inhibition of electron transport and mitochondrial-dependent ATP production. This has led to the widespread belief that targeting this pathway, including the

development of potential inhibitors of MCU, might be a robust strategy to block injury that occurs in a wide array of clinically important disease processes from ischemia to neurodegeneration [19,24].

Taken together, there is an long and extensive literature suggesting that dynamic alterations in mitochondrial calcium plays a central role in a wide range of physiological conditions from acute metabolic regulation to determining the threshold for cell death. Nonetheless, the vast majority of these studies have been hampered by the inability to directly alter *in vivo* mitochondria calcium uptake. While ruthenium red and some of its derivatives readily block MCU function, these agents cannot reliably enter cells, thus limiting this as an approach to dynamically regulate calcium uptake in intact tissues [25]. However, the recent identification of MCU provides a potential genetic approach to directly test many of these concepts. Here, we have generated and characterized mice lacking MCU expression to gain further insight into the role of mitochondrial calcium in mammalian physiology.

Results

MCU regulates calcium uptake

To determine the physiological functions of MCU, we constructed a mouse model using a gene trap strategy in which a retroviral trapping vector was integrated into the first intron of the *CCDC109A* locus (Supplemental Fig. S1a,b). While slightly smaller (Fig. 1a,b), organ weight was proportional to body size and overall body composition was indistinguishable between young and old *WT* and *MCU*$^{-/-}$ mice (Supplemental Fig. S1c,d). Further examination of *MCU*$^{-/-}$ embryonic and adult tissues by electron microscopy revealed no obvious abnormalities in mitochondrial number or morphology (Supplemental Fig. S2a). Although mice generated using a gene trap strategy sometimes leads to hypomorphic expression of the targeted gene, there was little evidence of *MCU* mRNA expression (Fig. 1c). Similarly, Western blot analysis using antibodies recognizing either N-terminal or C-terminal regions of the protein failed to detect any MCU protein expression in tissues derived from *MCU*$^{-/-}$ mice (Fig. 1d and Supplemental Fig. S2b,c).

We next sought to assess whether the absence of MCU expression altered mitochondrial calcium uptake. When purified mitochondria isolated from skeletal muscle of adult *WT* and *MCU*$^{-/-}$ mice were loaded with the calcium sensitive dye Fluo-4FF, wild type mitochondria exhibited robust calcium uptake over a range of physiological relevant extramitochondrial calcium concentrations (Fig. 1e). This uptake was inhibited in wild type mitochondria by the addition of the potent ruthenium red subcomponent, Ru360. However, *MCU*$^{-/-}$ skeletal muscle mitochondria, that lacked detectable MCU expression (Fig. 1e inset), exhibited no appreciable calcium uptake over a range of physiological calcium concentrations. Additional experiments performed with heart mitochondria revealed similar findings, although with cumulative additions of micromolar concentrations of calcium, we did note that *MCU*$^{-/-}$ cardiac mitochondria marginally increased their Fluo-4FF fluorescence (Fig. 1f), although this appeared to represent non-specific leakage of dye out of the mitochondrial matrix as indicated by rapid quenching of the fluorescent signal with EGTA (Supplemental Fig. S3a,b). We performed parallel experiments using Calcium Green-5N to measure extramitochondrial calcium levels (Fig. 1g). In these experiments, calcium addition to *WT*

cardiac mitochondria resulted in a rapid increase in Calcium Green-5N fluorescence followed by a slower decline in the fluorescence intensity of the calcium sensor (Fig. 1g). This slower decrease in fluorescence after calcium addition is consistent with the known buffering capacity of mitochondria to uptake cytosolic calcium. At higher concentrations of calcium (≥15 μM), buffering capacity is eventually exceeded and stored mitochondrial calcium is released into the extramitochondrial space. Over the same range of calcium concentration, *MCU*$^{-/-}$ mitochondria did not demonstrate evidence for either mitochondrial uptake or release.

To further analyze the function of MCU within intact cells, we generated primary mouse embryonic fibroblasts (MEFs) from *wild type* and *MCU*$^{-/-}$ embryos. Functional assessment revealed that when calcium was added to permeabilized MEFs, there was an initial rapid spike in Calcium Green-5N fluorescence intensity (Fig. 2a), which was followed by a slower decline in the fluorescence intensity of the cytosolic calcium sensor. As described above, this decline in fluorescence corresponds to mitochondrial calcium uptake. In permeablized wild type MEFs, in the presence of ER calcium uptake inhibition, mitochondrial uptake continued until the calcium retention capacity of the mitochondria was exceeded. At this point (e.g. the fourth addition of calcium in Fig. 2a), any further increase in extramitochondrial calcium resulted in a large rise in measured fluorescence. This terminal, large fluorescent increase indicates the irreversible release of mitochondria calcium stores and is commonly used as an index of PTP opening (similar to Fig. 1g). In contrast, calcium addition to *MCU*$^{-/-}$ MEFs resulted in a staircase profile consistent with the inability of *MCU*$^{-/-}$ mitochondria to rapidly uptake calcium (Fig. 2a). The profile seen in *MCU*$^{-/-}$ MEFs was similar to what is observed when wild type MEFs were treated with ruthenium red (Fig. 2b). Retroviral-mediated reconstitution of wild type MCU expression restored mitochondrial calcium uptake in *MCU*$^{-/-}$ MEFs (Fig. 2c,d). In contrast, a mutant of *MCU* where the critical acidic linker region was mutated at amino acid 261 and 264 was unable to reconstitute calcium uptake when expressed in *MCU*$^{-/-}$ cells.

To assess mitochondrial calcium uptake in a more physiological context, we isolated adult cardiac myocytes from *WT* and *MCU*$^{-/-}$ mice. Consistent with previous results[26], in *WT* myocytes loaded with the mitochondrial-targeted calcium sensitive dye Rhod-2 in the presence of manganese added to quench any cytosolic signal, isoproterenol addition stimulated a measurable rise in mitochondrial calcium levels (Fig. 3a). This response was absent in cardiac myocytes obtained from *MCU*$^{-/-}$ mice. Mitochondrial calcium levels were also unchanged in *MCU*$^{-/-}$ myocytes treated with agents (KCl and caffeine) that have been shown to directly increase cytosolic calcium (Supplemental Fig. S3c,d). Similarly, analysis of MEFs engineered to express a mitochondrial-targeted aequorin construct and then stimulated with histamine revealed that ligand-stimulated mitochondrial calcium fluxes were markedly diminished in *MCU*$^{-/-}$ cells (Fig. 3b). In contrast, histamine-induced cytosolic calcium changes were similar (Fig. 3c). Thus, as we observed with isolated mitochondria, cells derived from *MCU*$^{-/-}$ mice appear unable to rapidly uptake calcium.

MCU and metabolism

We next sought to ascertain the role of MCU in basal metabolism. Somewhat surprisingly, when we analyzed oxygen consumption of *MCU*$^{-/-}$ MEFs under basal conditions, we noted no detectable difference from *WT* MEFs using a variety of potential metabolic substrates (Fig. 4a and Supplemental Fig. S4a). This lack of a discernible difference may reflect the low basal energetic requirement for MEFs in culture, although treatment with mitochondrial membrane depolarizing agents such as FCCP, suggests *WT* and *MCU*$^{-/-}$ MEFs had a similar maximal oxidative capacity. To further pursue the absence or presence of a basal metabolic phenotype, we isolated mitochondria from *wild type* and *MCU*$^{-/-}$ mice. When purified mitochondria were given glutamate and malate as a substrate, we noted that *MCU*$^{-/-}$ and *wild type* mitochondria exhibited similar levels of respiration (Fig. 4b). Similarly, the response to ADP and the respiratory control ratio (State 3/State 4) were indistinguishable (Fig. 4b,c). Furthermore, metabolic assessment of total body basal oxygen consumption was not altered in *MCU*$^{-/-}$ mice (Fig. 4d). Finally, in contrast to what has been observed in cell culture models using primarily immortalized and transformed cells[27], we found no clear evidence of increased levels of autophagy in primary cells or tissues lacking MCU expression (Supplemental Fig. S4b,c). Taken together, these results demonstrate that basal metabolism is not markedly altered in the absence of MCU expression.

It has been known for nearly 50 years that calcium, similar to ADP and FCCP, can induce mitochondrial membrane depolarization and thereby transiently stimulate oxygen consumption[28]. Consistent with these past observations, in *WT* mitochondria, calcium addition resulted in nearly a 10-fold increase in mitochondrial respiration (Fig. 5a). In contrast, no calcium-dependent stimulation was observed in the respiration of mitochondria obtained from *MCU*$^{-/-}$ mice. While informative, such experiments using isolated mitochondria and high concentrations of calcium are by nature non-physiological. Thus, to better understand the physiological importance of mitochondrial calcium, we concentrated on the role of MCU in skeletal muscle physiology *in vivo*. One postulated effect of intramitochondrial calcium is the regulation of key mitochondrial enzymes involved in bioenergetics and metabolic flux. In particular, the phosphorylation of pyruvate dehydrogenase (PDH) is thought to be modulated by the calcium-sensitive phosphatase PDP1[29]. We reasoned that *MCU*$^{-/-}$ mice should allow a direct test of whether PDH is indeed regulated *in vivo* by these mechanisms. We first measured resting matrix calcium levels in mitochondria isolated from the skeletal muscle of *WT* and *MCU*$^{-/-}$ mice. We noted an approximate 75% reduction in basal matrix calcium levels in the mitochondria of *MCU*$^{-/-}$ mice (Fig. 5b). Using a phospho-specific PDH E1 subunit antibody, we next analyzed the level of PDH phosphorylation in three pairs of *WT* and *MCU*$^{-/-}$ mice. Consistent with the role for the calcium-sensitive phosphatase PDP1 regulating PDH phosphorylation, lower levels of matrix calcium in the *MCU*$^{-/-}$ mice led to markedly increased levels of PDH phosphorylation in the *MCU*$^{-/-}$ mice (Fig. 5c). We noted these changes across a variety of muscle types including skeletal muscle groups that were either fast twitch, slow twitch or mixed fibers (Fig. 5d). These phosphorylation differences were most evident under starved conditions and largely disappeared when the animals were re-fed (Supplemental Fig. S5a-c). Similarly, direct addition of calcium to *WT* mitochondria led to a rapid reduction in PDH E1 phosphorylation, a response not evident in isolated *MCU*$^{-/-}$ mitochondria (Supplemental Fig.

S5d). Previous results have indicated that this phosphorylation change on the E1 subunit is known to negatively regulate PDH activity[30]. Consistent with these past results, PDH activity was significantly reduced in the skeletal muscle of starved *MCU*$^{-/-}$ mice, while citrate synthase activity was not altered (Fig. 5e and Supplemental Fig. S5e). Finally, a decrease in PDH activity often correlates with a rise in serum lactate levels. We noted that *MCU*$^{-/-}$ mice indeed had a significantly elevated serum lactate level (Fig. 5f). Direct measurement of muscle lactate levels demonstrated a similar trend, while other TCA metabolites were not altered (Fig. 5g).

MCU regulates skeletal muscle work

The entry of calcium into the mitochondria during various physiological stresses is thought to increase mitochondrial energy production[11]. We next designed a number of functional tests that required a rapid increase in skeletal muscle work load. When we assessed skeletal muscle peak performance by placing mice on a rapid, steep treadmill, we observed a statistically significant impairment in the exercise capacity of *MCU*$^{-/-}$ mice (Fig. 6a). Similarly, when we assessed forearm grip strength, a measure of predominantly isometric muscle contraction, we also noted a small, but significant decrease in the strength of *MCU*$^{-/-}$ mice (Fig. 6b). This defect was more dramatic when we measured the ability of the mice to perform a pull up maneuver that requires concentric muscle contraction and hence increased power output (Fig. 6c). These observed defects in the ability of *MCU*$^{-/-}$ animals to generate maximal power output were not due to any apparent alterations in skeletal muscle fiber composition (Fig 6d and Supplemental Fig. S6).

The role of MCU in cell death

The opening of the PTP causes a rapid inflow of solutes inducing mitochondrial swelling and can be readily monitored by a number of approaches including a rapid fall in absorbance[31]. Consistent with previous results, the addition of extramitochondrial calcium to *WT* cardiac mitochondria induced PTP opening (Fig. 7a). For *WT* mitochondria, this opening was inhibited by addition of either cyclosporin A or Ru360. In contrast, *MCU*$^{-/-}$ mitochondria isolated from either liver or heart exhibited no evidence of PTP opening even after exposure to high levels of calcium for prolonged periods of time (Fig. 7a,b and Supplemental Fig. S7a). As such, these observations are consistent with our previous observations in permeabilized cells (see Fig. 2a) and demonstrate that MCU is required for calcium-induced PTP opening.

We next sought to understand the physiological importance of these observations. We took *MCU*$^{-/-}$ or *WT* MEFs and exposed them to a range of potential inducers of cell death. These agents included hydrogen peroxide as a prototypical example of oxidative stress, the ER stress inducing agent tunicamycin, the chemotherapeutic and DNA damaging agent doxorubicin, C2-ceramide an agent that can activate both apoptotic and necrotic pathways and thapsigargin, which triggers cell death by interfering with ER calcium uptake. We monitored cell death using the combination of annexin V and propidium iodine staining. While all of these agents were effective at inducing cell death, we noted no difference in the kinetics or magnitude of cell death in MEFs with or without MCU expression (Fig. 7c). We also noted that the release of cytochrome C from the mitochondria into the cytosol was not

affected by *MCU* expression, nor did we observe a significant difference in cytosolic calcium levels during cell death (Fig. 7d and Supplemental Fig. S7b,c). For both tunicamycin and doxorubicin we also measured the degree of Caspase-3 activity. Again, we noted indistinguishable levels of Caspase-3 activation in wild type and *MCU*$^{-/-}$ cells (Fig. 7e).

Finally, to assess whether similar effects were observed in tissues and organs, we subjected heart of *wild type* and *MCU*$^{-/-}$ mice to ischaemia-reperfusion (I/R) injury. When the degree of injury was assessed by functional measurements such as the post-ischemic recovery in the rate pressure product (RPP) or by pathological measurements such as direct assessment of the infarct area, our analysis revealed that *MCU*$^{-/-}$ mice exhibited no evidence for protection from I/R-mediated injury (Fig. 8a,b). Similarly, the level of apoptosis and the magnitude of ischemic contracture was equivalent in *WT* and *MCU*$^{-/-}$ hearts subjected to I/R injury (Supplemental Fig. S8a,b). Interestingly, while as expected the PTP inhibitor cyclosporin A (CsA) provided significant protection to *WT* hearts[32], this agent had no demonstrable effect on *MCU*$^{-/-}$ hearts (Fig. 8a,b).

Discussion

In summary, we provide the first *in vivo* description of the physiological effects seen in the absence of MCU expression. Remarkably, although mitochondria and cells from *MCU*$^{-/-}$ mice lack evidence for high capacity calcium uptake, these animals are grossly normal. While this result is somewhat unexpected, it should be noted that a previous study found no significant organ pathology following continuous siRNA-mediated knockdown of MCU in the liver[9]. Furthermore, few discernable phenotypes were observed in mice genetically deficient for myoglobin, creatine kinase or creatine, molecules that were all originally thought to be absolutely essential for cardiac and skeletal muscle bioenergetics[33-35]. Indeed, in the context of the whole animal, the absence of MCU produces relatively minor alterations in basal energetics. However, we should note that we found a significant reduction, but not a complete absence, of mitochondrial matrix calcium in mice lacking MCU. For instance, in our analysis, matrix calcium appeared to be reduced to about 25% of wild type levels in the skeletal muscle mitochondria of starved *MCU*$^{-/-}$ mice. This non-zero value suggests that alternative mechanisms must exist for calcium entry, although based on our cellular and isolated mitochondrial studies; the high capacity, rapid entry mode that occurs through the uniporter is clearly absent. It is conceivable that these slower and presumably low capacitance mechanisms might allow for some physiological adaptation over time.

We also observed that while *MCU*$^{-/-}$ mitochondria lacked evidence for calcium-induced PTP opening, the absence of MCU expression did not result in a demonstrable alteration in the magnitude of *in vitro* or *in vivo* cell death. Previous results with transient manipulation had suggested that altering MCU expression modulated the sensitivity to cell death in many [10,36] but not all[37] cellular systems. Interestingly, we observed that while the absence of MCU did not alter the magnitude of cell death, *MCU*$^{-/-}$ hearts were insensitive to CsA treatment. One interpretation is that in the absence of MCU, additional CsA-independent and calcium-independent cell death pathways emerge and predominate. Interestingly, yeast mitochondria

lack an MCU equivalent but still appear to undergo PTP opening, although this event appears to be insensitive to both calcium and CsA[38].

Finally, while there is unequivocal evidence for the *in vitro* regulation of mitochondrial dehydrogenase function by calcium[11], the observation that *MCU*$^{-/-}$ mice have limited defects in basal metabolism suggests that the *in vivo* effects of altering matrix calcium may be most important under certain stress conditions. Our results demonstrate that in tissues such as skeletal muscle, that exhibit a large dynamic energetic range, mitochondrial calcium regulates the intrinsic metabolism of the tissue as well as the peak performance. The observation that the defect in maximal skeletal muscle power output of MCU$^{-/-}$ mice is qualitatively similar to what was observed in mice deficient in creatine kinase[34] suggests that this property of skeletal muscle, i.e the ability to rapidly boost and maintain peak power output, is for obvious reasons, under intense evolutionary pressure.

Supplementary Material

Refer to Web version on PubMed Central for supplementary material.

Acknowledgments

We are grateful to C. Brantner, P.S. Connelly and M.P. Daniels of the NHLBI Electron Microscopy Core Facility for assistance with electron microscopy, C. Petucci of the Metabolomics Core Facility Sanford-Burnham Medical Research Institute for aiding in the metabolomic profiling, C. Combs and the NHLBI Microscopy Core for help with the Rhod-2 fluorescent measurements and A. Wiederkehr for the original mito-aequorin adenovirus. This work was supported by NIH Intramural funds.

References

1. Deluca HF, Engstrom GW. Calcium uptake by rat kidney mitochondria. Proc Natl Acad Sci U S A. 1961; 47:1744–1750. [PubMed: 13885269]
2. Vasington FD, Murphy JV. Ca ion uptake by rat kidney mitochondria and its dependence on respiration and phosphorylation. J Biol Chem. 1962; 237:2670–2677. [PubMed: 13925019]
3. Gunter TE, Pfeiffer DR. Mechanisms by which mitochondria transport calcium. Am J Physiol. 1990; 258:C755–786. [PubMed: 2185657]
4. Gunter TE, Sheu SS. Characteristics and possible functions of mitochondrial Ca(2+) transport mechanisms. Biochim Biophys Acta. 2009; 1787:1291–1308. [PubMed: 19161975]
5. Raffaello A, De Stefani D, Rizzuto R. The mitochondrial Ca(2+) uniporter. Cell Calcium. 2012; 52:16–21. [PubMed: 22672876]
6. Selwyn MJ, Dawson AP, Dunnett SJ. Calcium transport in mitochondria. FEBS Lett. 1970; 10:1–5. [PubMed: 11945343]
7. Kirichok Y, Krapivinsky G, Clapham DE. The mitochondrial calcium uniporter is a highly selective ion channel. Nature. 2004; 427:360–364. [PubMed: 14737170]
8. Moore CL. Specific inhibition of mitochondrial Ca++ transport by ruthenium red. Biochem Biophys Res Commun. 1971; 42:298–305. [PubMed: 4250976]
9. Baughman JM, et al. Integrative genomics identifies MCU as an essential component of the mitochondrial calcium uniporter. Nature. 2011; 476:341–345. [PubMed: 21685886]
10. De Stefani D, Raffaello A, Teardo E, Szabo I, Rizzuto R. A forty-kilodalton protein of the inner membrane is the mitochondrial calcium uniporter. Nature. 2011; 476:336–340. [PubMed: 21685888]
11. Denton RM. Regulation of mitochondrial dehydrogenases by calcium ions. Biochim Biophys Acta. 2009; 1787:1309–1316. [PubMed: 19413950]

12. Satrustegui J, Pardo B, Del Arco A. Mitochondrial transporters as novel targets for intracellular calcium signaling. Physiol Rev. 2007; 87:29–67. [PubMed: 17237342]
13. Territo PR, Mootha VK, French SA, Balaban RS. Ca(2+) activation of heart mitochondrial oxidative phosphorylation: role of the F(0)/F(1)-ATPase. Am J Physiol Cell Physiol. 2000; 278:C423–435. [PubMed: 10666039]
14. Balaban RS. Cardiac energy metabolism homeostasis: role of cytosolic calcium. Journal of molecular and cellular cardiology. 2002; 34:1259–1271. [PubMed: 12392982]
15. Hochachka PW, McClelland GB. Cellular metabolic homeostasis during large-scale change in ATP turnover rates in muscles. J Exp Biol. 1997; 200:381–386. [PubMed: 9050247]
16. Denton RM, McCormack JG. Ca2+ as a second messenger within mitochondria of the heart and other tissues. Annu Rev Physiol. 1990; 52:451–466. [PubMed: 2184763]
17. Glancy B, Balaban RS. Role of mitochondrial Ca2+ in the regulation of cellular energetics. Biochemistry. 2012; 51:2959–2973. [PubMed: 22443365]
18. Liu T, O'Rourke B. Regulation of mitochondrial Ca2+ and its effects on energetics and redox balance in normal and failing heart. J Bioenerg Biomembr. 2009; 41:127–132. [PubMed: 19390955]
19. Rasola A, Bernardi P. Mitochondrial permeability transition in Ca(2+)-dependent apoptosis and necrosis. Cell Calcium. 2011; 50:222–233. [PubMed: 21601280]
20. Rizzuto R, De Stefani D, Raffaello A, Mammucari C. Mitochondria as sensors and regulators of calcium signalling. Nat Rev Mol Cell Biol. 2012; 13:566–578. [PubMed: 22850819]
21. Orrenius S, Zhivotovsky B, Nicotera P. Regulation of cell death: the calcium-apoptosis link. Nat Rev Mol Cell Biol. 2003; 4:552–565. [PubMed: 12838338]
22. Lemasters JJ, Theruvath TP, Zhong Z, Nieminen AL. Mitochondrial calcium and the permeability transition in cell death. Biochim Biophys Acta. 2009; 1787:1395–1401. [PubMed: 19576166]
23. Spat A, Szanda G, Csordas G, Hajnoczky G. High- and low-calcium-dependent mechanisms of mitochondrial calcium signalling. Cell Calcium. 2008; 44:51–63. [PubMed: 18242694]
24. Hausenloy DJ, Yellon DM. Myocardial ischemia-reperfusion injury: a neglected therapeutic target. J Clin Invest. 2013; 123:92–100. [PubMed: 23281415]
25. Griffiths EJ. Mitochondrial calcium transport in the heart: physiological and pathological roles. Journal of molecular and cellular cardiology. 2009; 46:789–803. [PubMed: 19285504]
26. Chacon E, et al. Mitochondrial free calcium transients during excitation-contraction coupling in rabbit cardiac myocytes. FEBS Lett. 1996; 382:31–36. [PubMed: 8612759]
27. Mallilankaraman K, et al. MCUR1 is an essential component of mitochondrial Ca2+ uptake that regulates cellular metabolism. Nat Cell Biol. 2012; 14:1336–1343. [PubMed: 23178883]
28. Chance B. The Energy-Linked Reaction of Calcium with Mitochondria. J Biol Chem. 1965; 240:2729–2748. [PubMed: 14304892]
29. Karpova T, Danchuk S, Kolobova E, Popov KM. Characterization of the isozymes of pyruvate dehydrogenase phosphatase: implications for the regulation of pyruvate dehydrogenase activity. Biochim Biophys Acta. 2003; 1652:126–135. [PubMed: 14644048]
30. Holness MJ, Sugden MC. Regulation of pyruvate dehydrogenase complex activity by reversible phosphorylation. Biochem Soc Trans. 2003; 31:1143–1151. [PubMed: 14641014]
31. Blattner JR, He L, Lemasters JJ. Screening assays for the mitochondrial permeability transition using a fluorescence multiwell plate reader. Anal Biochem. 2001; 295:220–226. [PubMed: 11488625]
32. Hausenloy DJ, Boston-Griffiths EA, Yellon DM. Cyclosporin A and cardioprotection: from investigative tool to therapeutic agent. Br J Pharmacol. 2012; 165:1235–1245. [PubMed: 21955136]
33. Garry DJ, et al. Mice without myoglobin. Nature. 1998; 395:905–908. [PubMed: 9804424]
34. van Deursen J, et al. Skeletal muscles of mice deficient in muscle creatine kinase lack burst activity. Cell. 1993; 74:621–631. [PubMed: 8358791]
35. Lygate CA, et al. Living Without Creatine: Unchanged Exercise Capacity and Response to Chronic Myocardial Infarction in Creatine-Deficient Mice. Circ Res. 2013

36. Qiu J, et al. Mitochondrial calcium uniporter Mcu controls excitotoxicity and is transcriptionally repressed by neuroprotective nuclear calcium signals. Nat Commun. 2013; 4:2034. [PubMed: 23774321]

37. Curry MC, Peters AA, Kenny PA, Roberts-Thomson SJ, Monteith GR. Mitochondrial calcium uniporter silencing potentiates caspase-independent cell death in MDA-MB-231 breast cancer cells. Biochem Biophys Res Commun. 2013; 434:695–700. [PubMed: 23602897]

38. Jung DW, Bradshaw PC, Pfeiffer DR. Properties of a cyclosporin-insensitive permeability transition pore in yeast mitochondria. J Biol Chem. 1997; 272:21104–21112. [PubMed: 9261114]

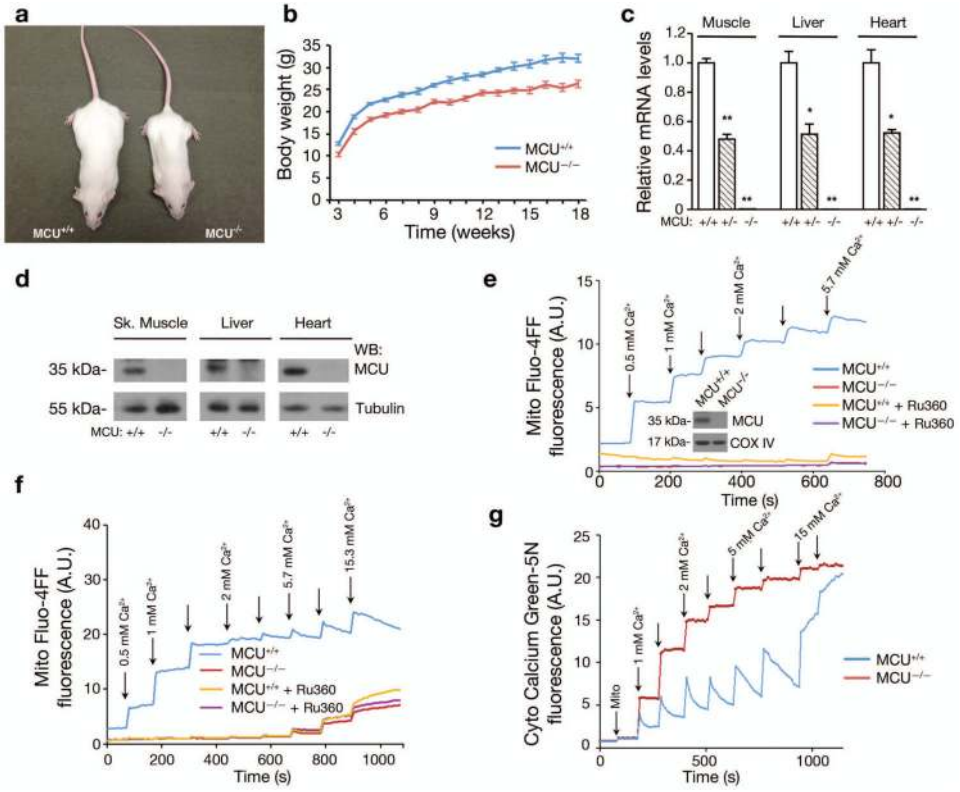

Figure 1.

MCU$^{-/-}$ mice lack MCU expression and evidence for rapid mitochondrial calcium uptake. **a**) Besides their size, *MCU*$^{-/-}$ mice (on right) lack a discernible phenotype. **b**) *MCU*$^{-/-}$ mice are smaller than WT mice (mean +/- S.E.M., p<0.01 by ANOVA; n=14 female *WT* and n=13 female *MCU*$^{-/-}$ mice). **c**) *MCU* mRNA expression by RT-PCR analysis in various tissues of *WT*, heterozygous and *MCU*$^{-/-}$ mice (n=3 animals per genotype, mean +/- S.E.M., *p<0.05, **p<0.01 by ANOVA compared to *WT* expression). **d**) MCU protein expression in various tissues using a rabbit polyclonal antibody generated against the C-terminus of MCU. Tubulin is used as a loading control. **e**) Assessment of mitochondrial calcium levels using the fluorescent mitochondrial calcium sensor Fluo-4FF. Calcium addition over the physiological (micromolar) range results in increasing calcium levels in mitochondria isolated from *WT* skeletal muscle. This uptake in *WT* mitochondria is inhibited by Ru360 addition. *MCU*$^{-/-}$ mitochondria lack any demonstrable uptake. Shown is one experiment that is representative of three similar experiments. Inset-Western blot analysis of MCU expression in purified *WT* and *MCU*$^{-/-}$ mitochondria with cytochrome C oxidase subunit IV (isoform 1) used as a loading control. **f**) Similar experiment performed using cardiac mitochondria. At higher Ca^{2+} concentrations, there is a small, non Ru360-inhibitable, increase in Fluo-4FF fluorescence in *MCU*$^{-/-}$ mitochondria observed. **g**) Parallel assessment of extramitochondrial calcium measurements demonstrating that only *WT* cardiac mitochondria appear capable of calcium uptake.

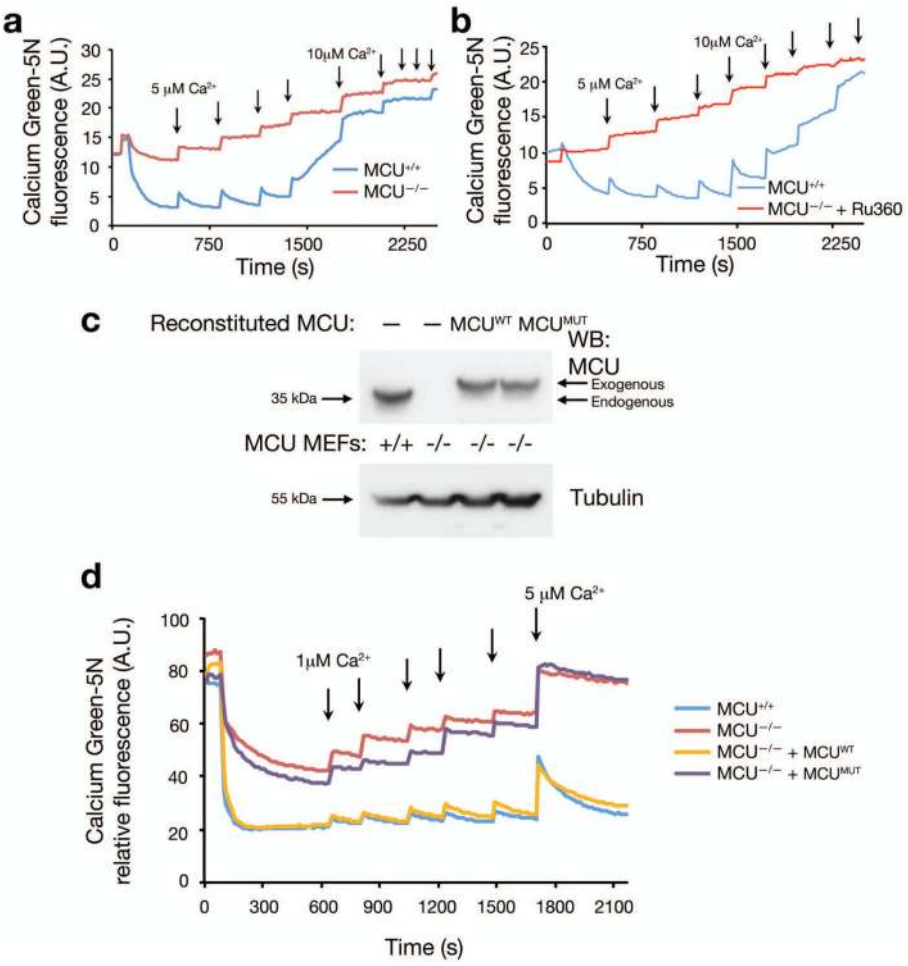

Figure 2.

MCU regulates mitochondrial calcium uptake in permeabilized MEFs. **a**) Comparison of cytosolic calcium levels in permeabilized *WT* and *MCU*$^{-/-}$ MEFs. Arrows indicate calcium addition. Increasing cytosolic calcium results in a rapid increase in the fluorescent signal in both cell types but the subsequent decline in the fluorescent signal, representing mitochondrial calcium uptake, is only observed in *WT* cells. Shown is one tracing that is representative of three similar experiments. **b**) Ruthenium red (Ru360; 3 μM) inhibits mitochondrial calcium uptake in permeabilized *WT* MEFs. **c**) Western blot analysis of MCU expression. *MCU*$^{-/-}$ MEFs were infected with retroviruses encoding an epitope-tagged form of either WT *MCU* or *MCU*^{mut} containing two amino acid substitutions (at amino acid 261 and 264) known to abrogate uniporter activity. The tagged constructs migrate slightly slower than endogenous MCU but were expressed at roughly endogenous levels. **d**) Cytosolic calcium measurements in permeabilized *WT* MEFs, *MCU*$^{-/-}$ MEFs, *MCU*$^{-/-}$ MEFs reconstituted with wild type MCU and *MCU*$^{-/-}$ MEFs reconstituted with MCU^{mut}.

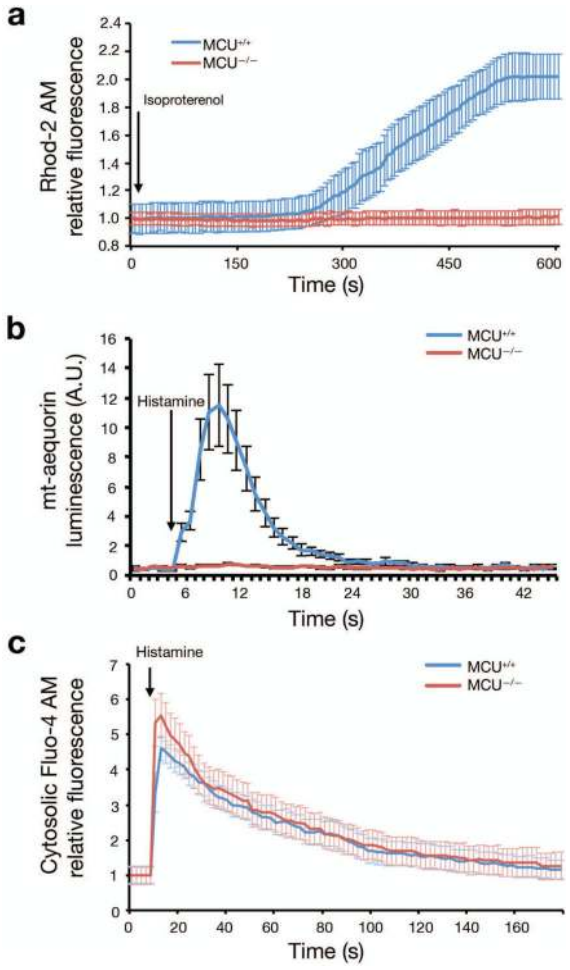

Figure 3.

MCU regulates ligand-stimulated mitochondrial calcium uptake. **a**) Isoproterenol stimulates an increase in mitochondrial calcium in *WT* cardiac myocytes. Adult *WT* and *MCU*$^{-/-}$ adult cardiac myocytes were freshly isolated, loaded with mitochondrial calcium sensitive probe Rhod-2 and stimulated with 1 μM isoproterenol at time zero (n=10 random fields per genotype). **b**) *WT* or *MCU*$^{-/-}$ MEFs were infected with an adenovirus encoding a mitochondrial targeted aequorin construct. Levels of mitochondrial calcium were assessed by aequorin luminescence following histamine stimulation (100 μM) for *WT* (n=10) and *MCU*$^{-/-}$ MEFs (n=12). Values were normalized to maximal aequorin luminescence observed in permeabilzed cells exposed to exogenous calcium. C) Cytosolic calcium levels in *WT* (n=14) or *MCU*$^{-/-}$ MEFs (n=17) as measured by Fluro-4 fluorescence following histamine stimulation. All pooled data represents mean +/- S.E.M.

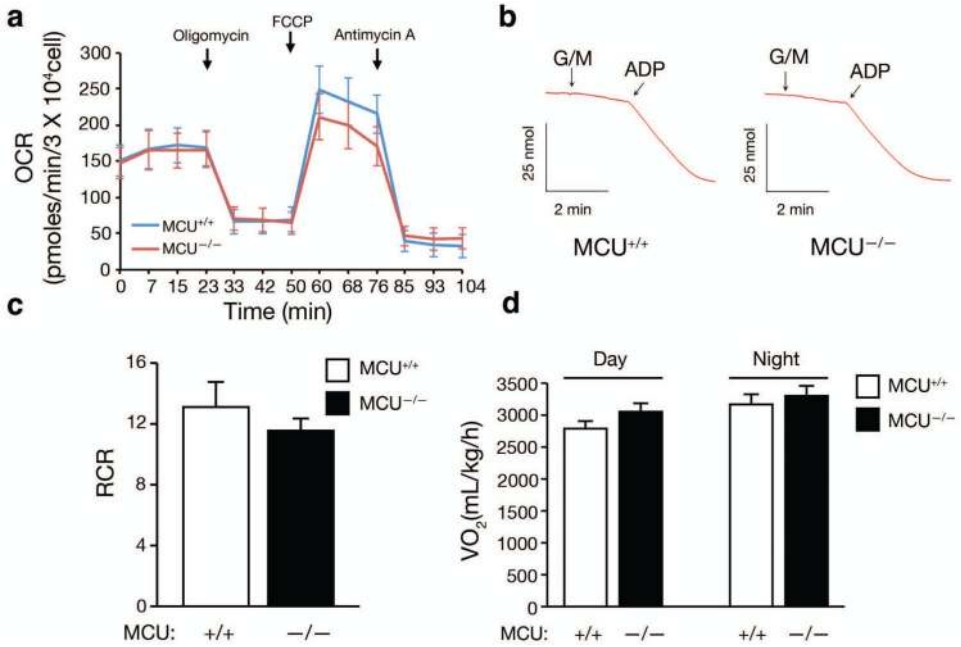

Figure 4.

The role of MCU in basal metabolism. **a**) Seahorse X-24 analysis of oxygen consumption rate (OCR) in *WT* and *MCU*$^{-/-}$ MEFs under basal conditions or following the addition of oligomycin, the uncoupler FCCP or the electron transport inhibitor antimycin A (n=5). **b**) Representative tracings of the oxygen consumption observed in isolated hepatic mitochondria given glutamate/malate as a substrate (G/M) followed by ADP (State 3). **c**) Quantification of the respiratory control ratio (RCR; State 3/State 4 respiration) in *WT* and *MCU*$^{-/-}$ mitochondria (p=NS; n=3 independent experiments). **d**) Average total body oxygen consumption in *WT* and *MCU*$^{-/-}$ mice during day and night conditions (n=5 *WT* and n=6 *MCU*$^{-/-}$ mice; p=NS between genotypes). All pooled data represents mean +/- S.E.M.

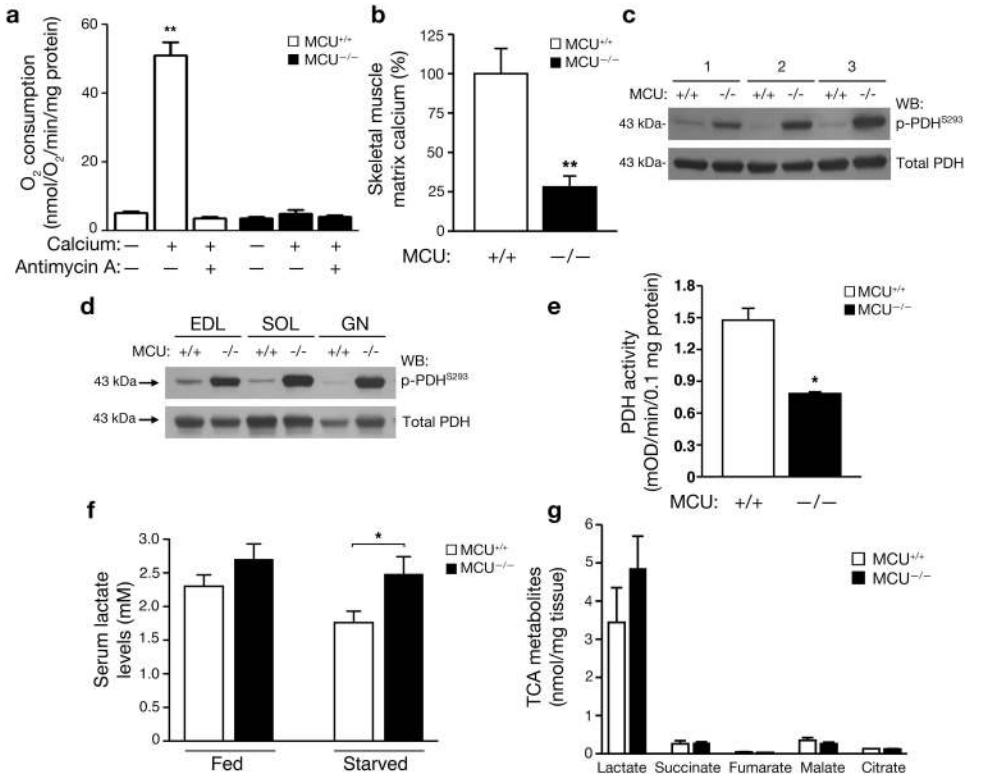

Figure 5.

Altered *in vivo* skeletal muscle metabolism and PDH activity in *MCU*$^{-/-}$ mice. **a**) Mitochondrial oxygen consumption following depolarization induced by the addition of 500 μM calcium with and without the respiratory chain inhibitor Antimycin A (15 μM). The average +/- SEM of three independent experiments is shown. **p<0.01 by t-test compared to without calcium. **b**) Levels of matrix calcium measured in *WT* and *MCU*$^{-/-}$ mitochondria derived from skeletal muscle following an overnight 16 hour fast (**p<0.01 by t-test; n=3 WT and N=4 MCU$^{-/-}$ mice). **c**) Western blot determination of the levels of phospho-PDH (serine 293 of the E1-α subunit) and total PDH levels in the skeletal muscle of three pairs of WT and MCU$^{-/-}$ mice starved for 16 hours. **d**) Under starved conditions, altered PDH phosphorylation is seen various muscle types including the extensor digitorum longus (EDL) representing glycolytic/fast twitch fibers, the soleus (SOL) that is predominantly oxidative/ slow twitch and the gastrocnemius (GN) that is a mix of fast and slow twitch. **e**) Skeletal muscle PDH activity in *WT* and *MCU*$^{-/-}$ mice after a 16 hour fast (*p< 0.05; n=3 mice per genotype). **f**) Serum lactate levels in *WT* and *MCU*$^{-/-}$ male mice under fed conditions or after 16 hours of starvation (n=7 WT and n=6 MCU$^{-/-}$, *p<0.05 by t-test). **g**) Metabolomic analysis of skeletal muscle demonstrating levels of various TCA cycle intermediates in mice that were starved overnight (n=3 per genotype). There was a trend for increased lactate levels in the *MCU*$^{-/-}$ muscle. All pooled data represents mean +/- S.E.M.

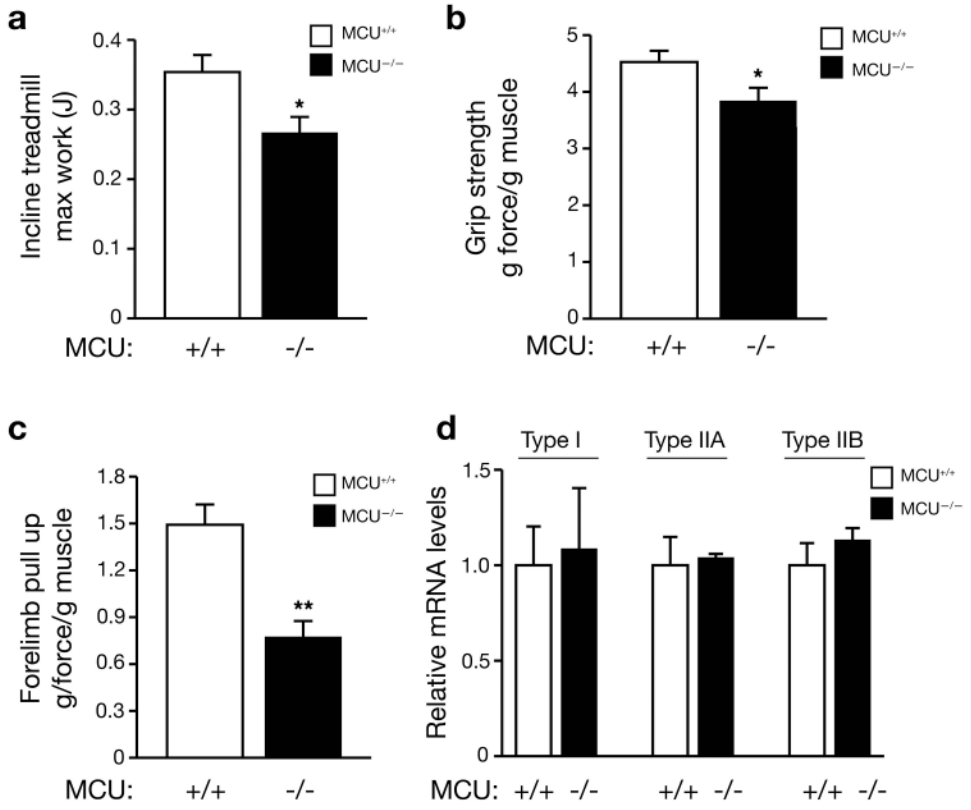

Figure 6.

MCU regulates skeletal muscle peak performance. **a**) Assessment of skeletal muscle function using maximal work performed on an inclined treadmill test (n=6 *WT* and n=11 *MCU*$^{-/-}$ mice). **b**) Grip strength assessment for *WT* and *MCU*$^{-/-}$ mice (n=5 *WT* and n=5 *MCU*$^{-/-}$ mice). **c**) Forelimb strength during a modified vertical pull up test (n=11 *WT* and n=12 *MCU*$^{-/-}$ mice). All mice assessed for physiological responses were female. *p<0.05 and **p<0.01 by t-test. **d**) Analysis of fiber-specific mRNA abundance in the gastrocnemius of *WT* and *MCU*$^{-/-}$ mice (n=3 mice per genotype, p=NS between genotypes). All pooled data represents mean +/- S.E.M.

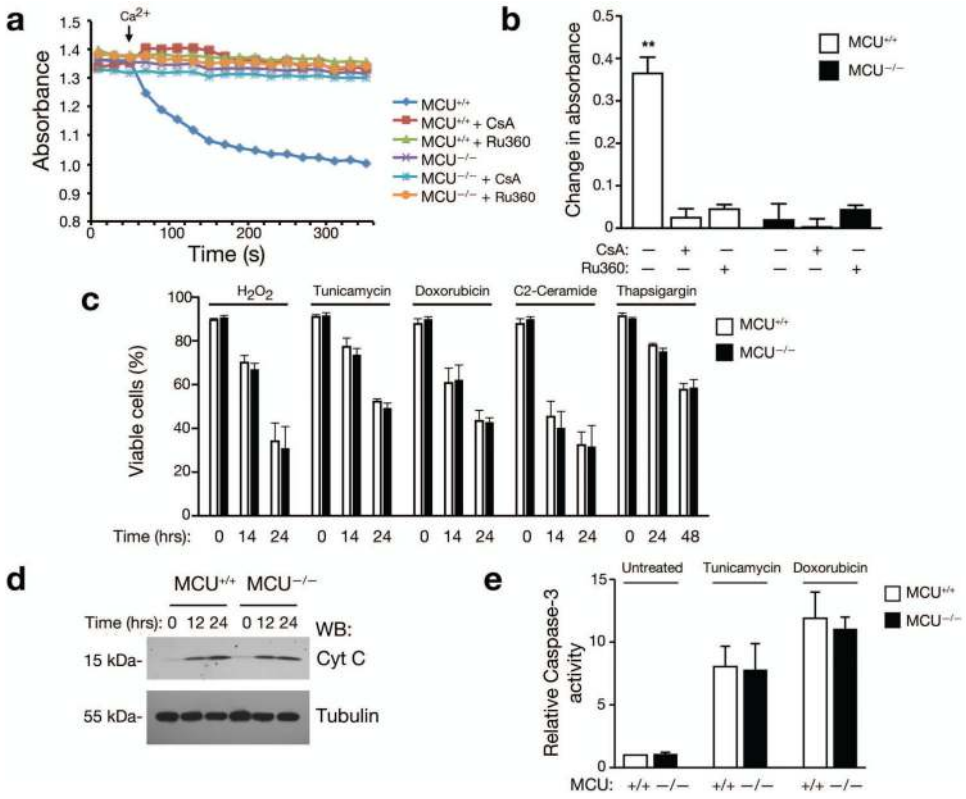

Figure 7.

MCU expression is necessary for calcium-induced PTP opening but not required for cell death. **a**) Only *WT* mitochondria undergo PTP opening after calcium addition (500 μM) as evidence by a rapid drop in absorbance. Shown is one experiment using heart mitochondria that is representative of three similar experiments. **b**) Average change in absorbance from three independent experiments using isolated cardiac mitochondria in the presence or absence of CsA (0.2 μM) and Ru360 (3.0 μM). **c**) Cell viability as measured by Annexin V/PI staining in *WT* and *MCU*$^{-/-}$ MEFs following a wide array of challenges including hydrogen peroxide exposure (1 mM), tunicamycin (2 μg/ml), doxorubicin (2 μM), C2-ceramide (100 μM) and thapsigargin (1 μM). The time course and magnitude of cell death was not altered by the absence of MCU expression (p=NS, n=3 per genotype). **d**) Cytosolic cytochrome C levels in *WT* or *MCU*$^{-/-}$ MEFs following the addition of hydrogen peroxide. Tubulin is shown as a loading control. **e**) Caspase-3 activity was measured under basal conditions or 24 hours after treatment with tunicamycin or doxorubicin (p=NS; n=3). All pooled data represents mean +/- S.E.M.

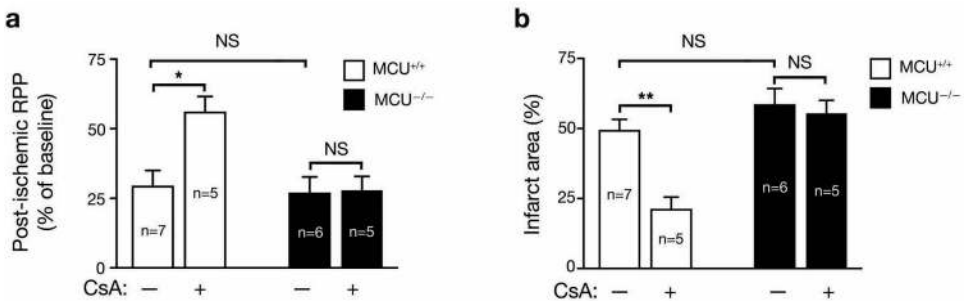

Figure 8.

Role of MCU in ischaemia-reperfusion injury. **a**) Assessment of the rate pressure product (RPP, heart rate times systolic blood pressure) after ischaemia-reperfusion injury in the hearts of *WT* or *MCU*$^{-/-}$ mice with and without Cyclosporin A (CsA, 0.2 μM) for five minutes prior to ischemia. **g**) Infarct size in *WT* and *MCU*$^{-/-}$ mice following 20 minutes of global ischemia and 90 minutes of reperfusion. *p<0.05, **p<0.01 by ANOVA; all pooled data represents mean +/- S.E.M.